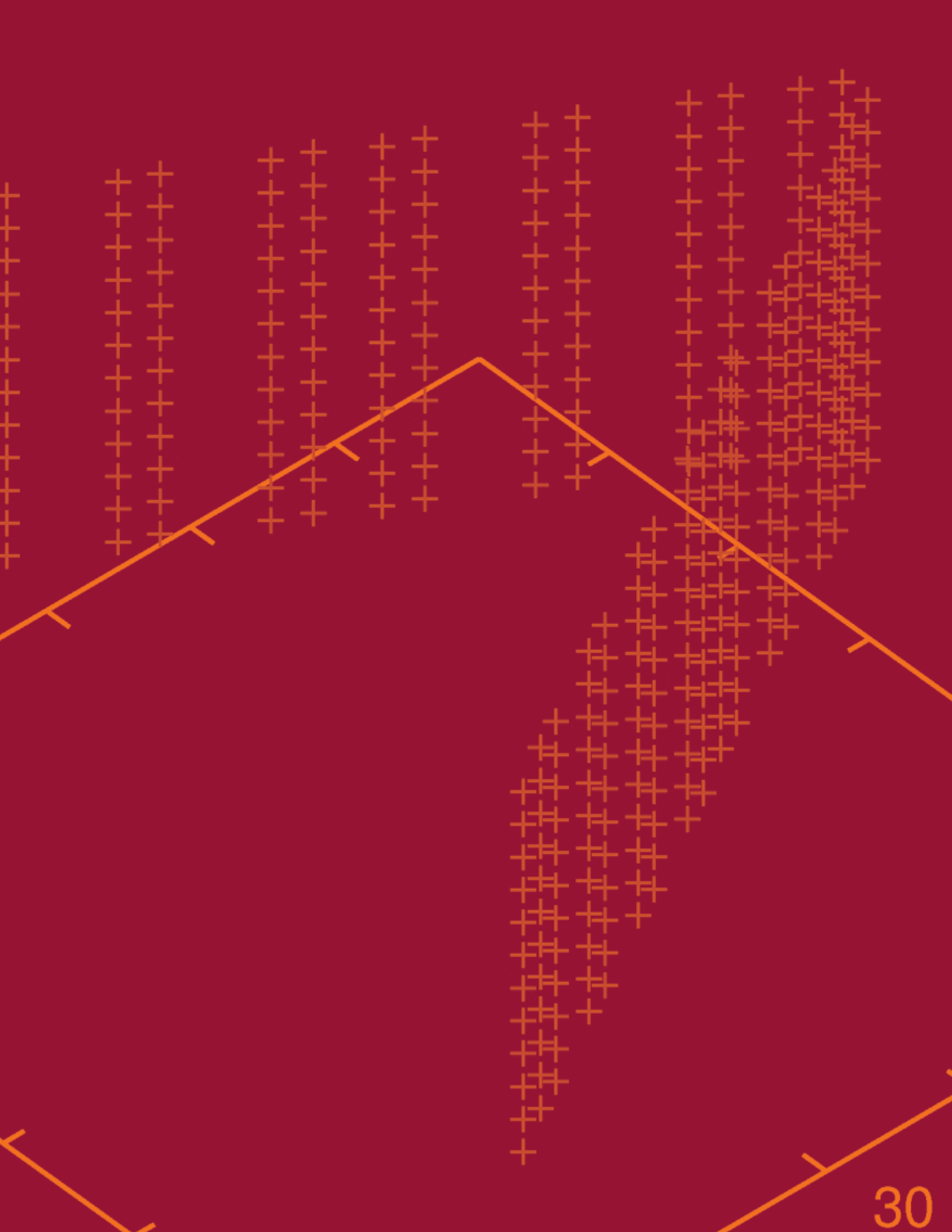

Electrodynamics Calculations of SMSERS Active Junctions and New UV Active Substrates

Undergraduate Researcher
Benjamin J. Faber
Fort Hays State University

Faculty Mentor
George C. Schatz
Department of Chemistry
Northwestern University

Post Doctoral Mentor
Jon P. Camden
Department of Chemistry
Northwestern University

Abstract

This research explored the optical properties of metal nanoparticles using the discrete dipole approximation (DDA). A method was developed to define nanoparticle structures of arbitrary shapes, and this method was interfaced with the preexisting DDA code, DDSCAT 6.1. For each structure and material, the scattering properties and near electric-field enhancements were calculated, which are important for predicting the intensity of surface-enhanced Raman scattering (SERS). Aluminum nanostructures exhibited UV and near-UV plasmon resonances and electric-field enhancements up to 10^3. Palladium exhibited enhancements of only 90. A dimer structure consisting of a silver sphere and a rod exhibited enhancements up to 105, which are large enough to observe single-molecule SERS.

Introduction

The optical properties of noble metal nanoparticles are a topic of much interest in nano-optics. One important optical property of noble metals is their ability to support localized surface-plasmon resonance (LSPR), which results from the response of the metal's conduction electrons to incident electromagnetic waves. The LSPR response of a small metal particle makes phenomena such as surface-enhanced Raman scattering (SERS) possible. Raman-scattered light is a type of inelastic light scattering in which a photon undergoes a shift in frequency upon absorption and subsequent reemission from an atom or molecule. Raman-scattered light can be very useful in the study of nanoscale objects because it provides chemical information on the surface-adsorbed species. SERS has the potential to be a powerful tool in fields ranging from nano-optics to microscopy, spectroscopy, and chemical and biological sensing.[1–3]

Raman-scattered light is difficult to observe because of the infrequency of occurrence and its relative weakness in intensity compared with elastically scattered light.[1] One solution to this problem is SERS. SERS is accomplished through two mechanisms: a chemical enhancement and an electromagnetic enhancement. Since most of the enhancement comes from the electromagnetic factor, this research focused on the use of electromagnetic enhancement to achieve SERS.

There are also two different types of enhancements with electromagnetic waves: the enhancement of the local electric field around the particle and the Raman enhancement. The local enhancement scales as the square of the electric field, but the Raman enhancement scales as the electric field to the 4^{th} power. Throughout this work, "enhancement" refers to the local enhancement, unless otherwise stated. The electromagnetic mechanisms work through the enhancement of the local electric field, which projects over the near-field region. Using a particle's LSPR is one way to enhance the localized electric field of a particle or substrate.[2] LSPR occurs when the conduction electrons of a metal are driven into oscillations by the electric-field component of the incident light beam at a wavelength corresponding to the resonance of the particle. The individual electric fields produced by the oscillating electrons then interact to enhance the localized electric field of the nanoparticle.

Recently there has been interest in single-molecule SERS (SMSERS).[1] Regular SERS can be observed for local enhancement factor as small as 10^2. However, SMSERS requires EM enhancement of ~10^{10}, which is difficult to achieve consistently. The wavelength at which LSPR occurs on a given particle is governed by: the particle geometry, composition, and dielectric material; the substrate on which the particle is resting; and the external solvent.[2] Previous work has been done on substrate and external medium effects of Au and Ag nanoparticles,[2,3] but little has been done in the field of geometry and composition. This research focused on the effects of particle geometry and local environment on the optical properties, and specifically on the extinction, scattering, and absorption spectra, and local electric-field enhancement. It also focused on electrodynamics calculations to determine the best shape, substrate, and medium for LSPR to occur and therefore to increase the use of SERS.

Background

The problem of light scattering off small particles has been a question in electrodynamics for the past century. Electrodynamics is governed by a set of four equations, known as Maxwell's equations.[4] In his groundbreaking paper, Mie solved Maxwell's equations exactly for a spherical particle.[4,5] Work to find exact solutions to Maxwell's equations for more arbitrarily shaped particles has had limited success. To date, exact solutions using Maxwell's equations are only possible with simple particle models, such as rectangular solids and cubes or spheroids. Hence, an approach that numerically approximates the solution with a high degree of accuracy is needed. For this study, the discrete dipole approximation, a method initially developed by Purcell and Pennypacker[6] in 1975, was chosen for reasons explained in the next section. This method has been used in a variety of different applications, ranging from scattering light off small particles that closely resemble laboratory-fabricated particles to approximating the optical spectrum of ice crystals in the upper atmosphere.[7]

The Raman effect was first observed experimentally in the 1920s,[8] setting off a significant amount of experimental research to measure and find applications for Raman-scattered light. The SERS field has made great progress, and recent experimental work has yielded fantastic results. It was found that the field enhancements necessary for SMSERS were best obtained through colloidal configurations and dimer structures.[3] Following this train of thought, the work of Micic and coworkers[9] achieved an enhancement factor of 10^5 through the interaction of an atomic force microscope tip and a spherical nanoparticle. In a more practical study, Xu and Käll et al.[10] showed that the enhancement factor of hemoglobin particle configurations was as large as 10^5. At that time, however, the technological limitations in imaging and particle fabrication prevented researchers from knowing the exact particle geometry. The advent of techniques capable of producing particles with known geometry enabled researchers to make headway toward finding accurate SERS substrates with large enhancement factors.

Approach

Solving Maxwell's equations for arbitrary particles leads to many different approaches, each with its own strengths and weaknesses. Over the years, three main methods of solving Maxwell's equations have evolved: the T-matrix, the modified long-wavelength approximation (MLWA), and the discrete dipole approximation (DDA).[11,12]

The T-matrix method provides exact numerical solutions to Maxwell's equations, but it is computationally intensive and inefficient. The MLWA, based on the solution of Maxwell's equations as the wavelength goes to infinity, is much simpler and easier to solve. The results of MLWA for spheres and spheroids where the eccentricity is relatively small match the results obtained by the T-matrix method very well. MLWA fails, however, when the spheroid becomes highly oblate.[11] Consequently, light scattering off more irregularly shaped particles cannot be modeled with MLWA.

DDA is one method that satisfies both requirements. It breaks up the target into a cubic lattice, with each point of the cubic lattice representing a dipole. More complex particles are easily defined as an exercise in three-dimensional geometry. Each dipole has a distinct polarizability, allowing it to interact with every other dipole in the lattice. DDA uses the cubic-lattice approach to model the oscillatory response of the conduction band electrons and the effect on the optical properties of the particle.[7] A rigorous explanation of the derivation and solution to the set of matrix equations obtained from DDA can be found in an excellent treatise by Draine.[13] A concern is that DDA is solving a eigenvector equation with matrix dimensions $3N \times 3N$ and vector dimensions $3N$, where N is the number of dipoles. The current program to run DDA (DDSCAT 6.1 by Draine and Flatau[14]) uses Fast Fourier Transforms to solve the equations, which speeds up the computing process considerably. DDA provides an efficient way of theoretically calculating the optical properties of nanoparticles that is not limited to simple geometric shapes.

Just as finding the peak of maximum extinction is important to find the wavelength at which LSPR occurs, finding the electric-field enhancement of the nanoparticle is necessary to determine whether it is a viable particle for SERS. The DDA routine in this study was useful because it calculated the necessary values to find the electric-field enhancement. Code developed by Li and Schatz took these quantities (which are both real and imaginary) and determined the enhancement, which was simply a multiple of the field values and their complex conjugates. The code outputs data on a series of planes in the direction specified by the user, and in the format to be used by the PLOTMTV program.

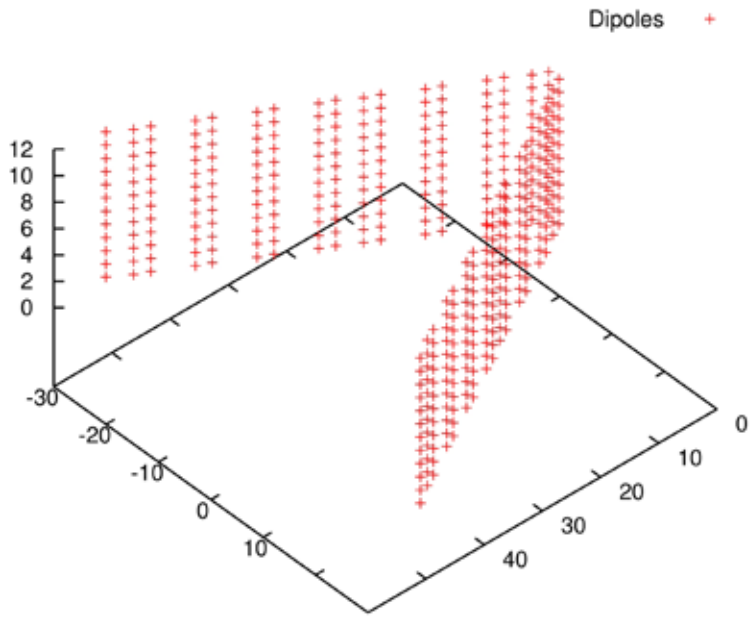

Figure 1. Dipole comparison of a triangular prism with an equilateral face of side length 60 nm and a thickness of 12 nm and a dipole spacing 1 nm between the user generated input files and the supplied DDA input files. The DDA code leaves off dipoles on the edges of the prism.

Additionally, the code finds the particle coordinates and the maximum field enhancement.

Results

Much of this research was devoted to devising ways to represent arbitrarily-shaped particles in terms of discrete dipoles and to use DDA to calculate the optical spectra. Hence, the first step was to ensure that DDA calculations matched Mie theory with extreme accuracy. DDA, as used in standard implementation,[14] contains a calculation to generate spheres and spheroids. A series of tests were run to compare DDA to Mie theory. The results found that optical spectra generated by the DDA preprogrammed routine and the code used in Mie theory[5] (exact solution) are almost identical. Analysis showed that DDA does not divide up the wavelengths evenly over the range of desired wavelengths, but stresses shorter wavelengths, leading to a decrease in accuracy when the wavelength gets larger. Despite this, the error between the two methods is almost negligible for the purpose of this work.

DDA functions by putting all locations of the dipoles in the problem space and their respective dielectric flags (i.e., 1 or 2, depending on whether 1 or 2 dielectric functions were used) in an input file. DDA is programmed to use "shape files" in standard implementation,[14] and it comes preprogrammed with several rudimentary shape functions. These rudimentary shapes were not of much interest to this work because many cannot be fabricated in the lab. New programs had to be written to generate these shape files. As a test case, a new program was written to generate a dipole file of the same shape that already could be made with DDA. Analysis of the shape file found that the two correlated almost exactly except along the edges. The new shape had more dipoles on the edges than did the DDA-generated shape, which is shown in Figure 1. The extra dipoles were still within the boundaries of the physical shape, which meant that the new shape was more accurate than the standard DDA implementation shape because of an increase in dipoles representing the target. The results of the two shapes were quite similar when used to calculate optical spectra. The preliminary shape was correct, and more complicated shapes could be constructed with confidence.

Much work has been done on the optical properties of silver nanoparticles and the resulting electric-field enhancements.[2,3,12] However, there are reasons, such as expense and chemical properties, to examine less-rare metals. One focus of this work was to examine the optical response of aluminum and palladium nanoparticles, which are of interest because of their role as catalysts and possible UV applications. All particles used in the DDA calculations are models of particles that can be fabricated in the laboratory, using a photosynthetic technique for the triangular prisms[15] (which has only proved possible for Au and Ag so far) or

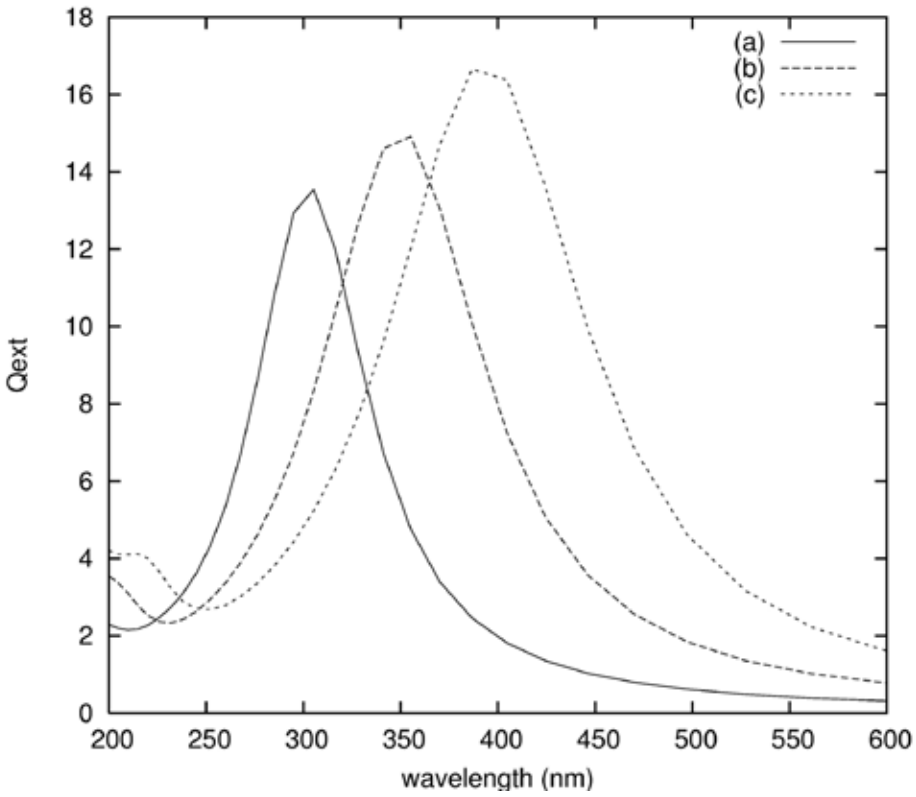

Figure 2. Plot of extinction values for Al triangular prisms. All particles have equilateral triangular faces and a thickness of 12 nm. (a) has a face side of 60 nm, (b) has a face side of 80 nm, and (c) has a face side of 100 nm.

nanosphere lithography (NSL)[2,12] for the truncated tetrahedrons. For the dielectric functions, the values for gold and silver were taken from the work of Johnson and Christy.[16] The aluminum and palladium values were drawn from the *CRC Handbook of Chemistry and Physics*.[17]

The right-triangular prism nanoparticle is of particular interest in the study of LSPR. The prism scatters light anisotropically, meaning it does not scatter light evenly in all directions. This is crucial to supporting a large LSPR. In the previous studies with silver nanoparticles, it was shown that there are "hot spots"[1] on the triangular prisms that have an extremely large electric-field enhancement when the particle is irradiated at the plasmon resonance. Results from this work were compared with those of Hao and Schatz,[3] who have examined silver in depth. The initial calculations in this research used the dimensions outlined in the Hao and Schatz paper. The dimensions of the prism are an equilateral triangular face with side length 60 nm and thickness 12 nm. Figure 2(a) gives the extinction spectrum of the 60 nm aluminum prism. The extinction spectrum of aluminum has a sharp peak at about 300 nm the ultraviolet range. The wavelength at which the LSPR of the prism occurs is the peak. In order to make aluminum a plasmonic material in the visible region of the spectrum, the peak of the extinction spectrum needs to be shifted about 100 nm to the red. Previous literature[3] suggests this can be accomplished by making the sides of the triangular face longer and the thickness of the prism smaller. It is not practical to try to make the already small thickness any smaller in the lab. By lengthening the sides of the triangular face to 100 nm, the extinction peak of the aluminum shifted from 300 nm to ~390 nm, extremely close to the visible light range (Figure 2(c)). When the electric-field enhancement of the aluminum prisms was calculated at the plasmon peak, it was found to be on the order of 10^3.

Palladium showed less promising results as an active SERS particle. The extinction maximum of palladium was tunable throughout the visible spectrum, with the reddest peak close to 500 nm. As seen in Figure 4, however, it was very broad, which led to an electric-field enhancement that was relatively small, about 100, compared with the other metals. The position of the maximum electric-field enhancement was crucial. SERS occurs only if the target is at one of these hot spots. On the triangular prisms, Figure 5 shows that the maximum field enhancement for aluminum occurs at one of the tips of the prism and at the leading triangular face of the prism. This means the target molecule must be delivered to this specific location, which is difficult with available technology.

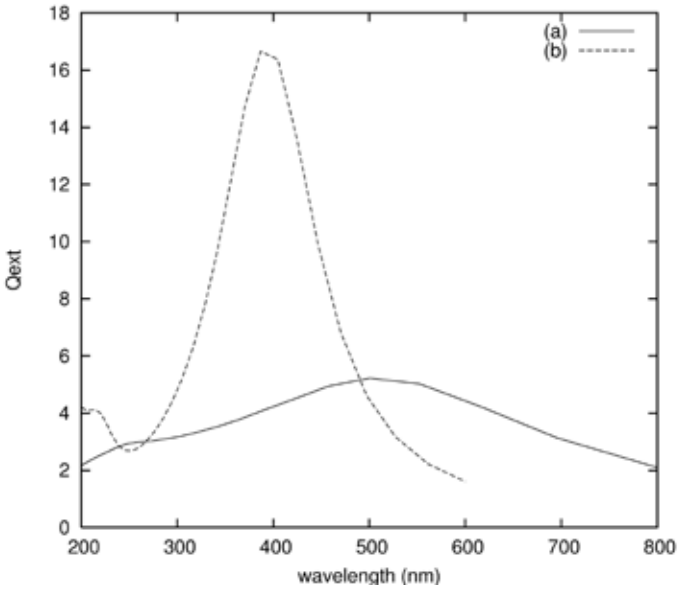

Figure 3. Extinction plot of (a) Pd triangular prism with equilateral face side lengths 100 nm and thickness 12 nm and (b) Al triangular prism of the same dimensions.

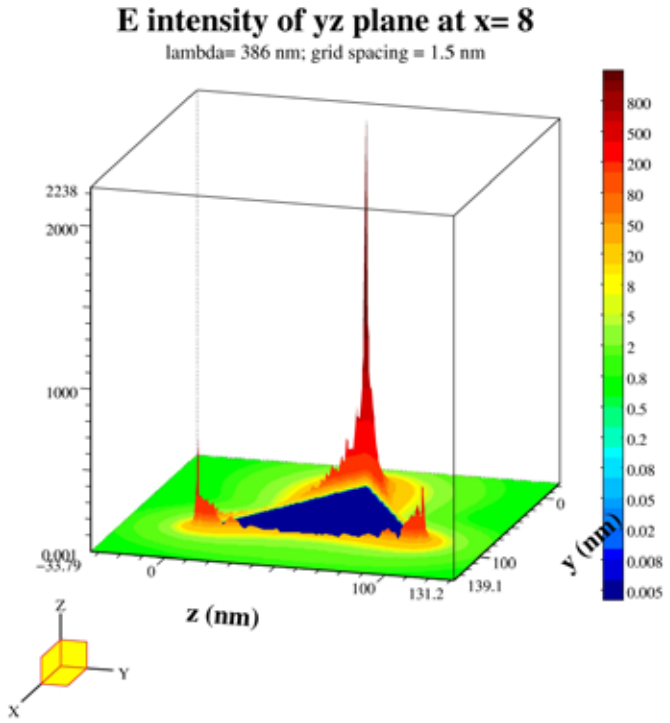

Figure 4. The electric field intensity of an Al triangular prism with a 100 nm face side. The position of the plane is at the end of the prism, x = 12 nm. The dipole space is 1.5 nm. Maximum electric field intensity is 2386.

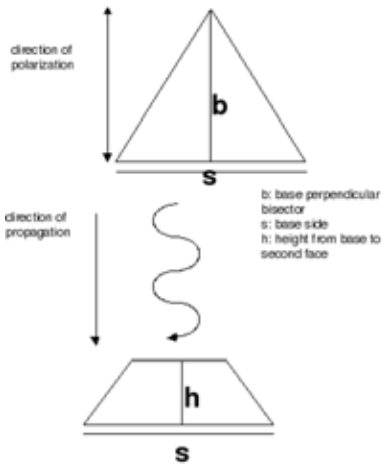

Figure 5. A schematic of the set-up for the truncated tetrahedrons. The aspect ratio of a truncated tetrahedron is b:h.

Truncated tetrahedrons can be made with high accuracy using the NSL technique,[2,12] which makes them important to the study of the optical properties of metal nanoparticles. All of the truncated tetrahedrons tested in this research were regular tetrahedrons, with the top cut off somewhere. For consistency, the polarization of the light was always parallel to a perpendicular bisector of the triangular face. The incident light was perpendicular to the smaller face of the tetrahedron (Figure 6). The tetrahedron's dimensions were changed two different ways: the side-to-height ratio and the base perpendicular bisector-to-height ratio (also know as the aspect ratio). Both silver and aluminum exhibited similar shifting properties. When comparing the silver with the aluminum tetrahedrons, the silver tetrahedron was further to the red end of the spectrum than the aluminum, a result consistent with that of the triangular prisms. Again, as with the triangular prisms, the plasmon resonance of the truncated tetrahedrons was tunable. By keeping the aspect ratio constant (Figure 7), the particle's LSPR red shifted as the bisector length increased and the height increased. This result differs significantly from those for the triangular prisms, which could be red-shifted by increasing the ratio of side length to thickness. The maximum extinction value of the tetrahedrons, however, was much greater than that of the prisms for all sizes tested. Analysis of the electric-field enhancement produced results similar with those of the triangular prisms. Figure 8 demonstrates that the hot spots for field enhancement lie at one of the vertexes of the base triangular face. The field enhancement is promising, sometimes as much as 10^4.

Dimer configurations of nanoparticles are known to produce much greater electric-field enhancements than do monomers.[3] SMSERS is possible only if there is a large-enough localized electric-field enhancement. It is imperative to know the geometry and configuration of nanoparticles for optimal electric-field enhancement. Van Duyne and coworkers have been able to image nanoparticle aggregates that give rise to SMSERS. In this work, the experimental structure was modeled and the size of the electric-field enhancement was determined. The theoretical electric-field enhancement can be calculated if the geometry of the particles can be accurately generated for use in DDA. Thus, the largest challenge in finding the field enhancement was generating the correct shape files for each of the particles. A tunneling electron microscope was used to determine physical measurements of the particles. These measurements were used to calculate an approximate geometry of all the particles. The particle thought to be SMSERS-active had well-measured dimensions. Figure 8 shows the dipole file for the dimer configuration. It consists of a rod with a hemisphere on each end directly adjacent to a sphere that is slightly offset from the center of the rod. The whole configuration sits on top of a substrate. The rod part of the dimer had a radius of 51 nm and a distance of 38 nm between the end hemispheres. The spherical portion sticking off the rod had a radius of 64 nm, and its center was offset 4 nm from the center of the rod. Two different polarizations were used for calculations — one polarization defined and the other orthogonal to the defined polarization (Figure 8).

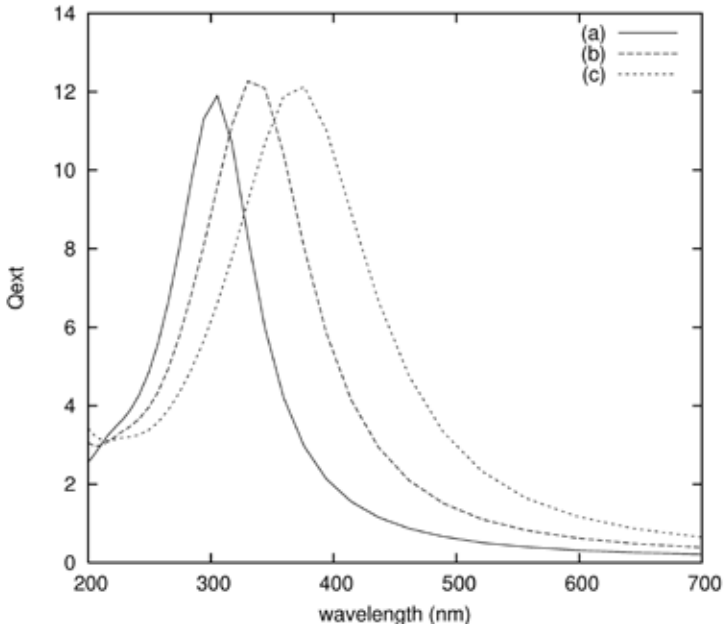

Figure 6. Plot of extinction values for truncated Al tetrahedrons. The aspect ratio is 4:1. (a) has a perpendicular bisector of 60 nm, (b) has a perpendicular bisector of 80 nm, and (c) has a perpendicular bisector of 100 nm.

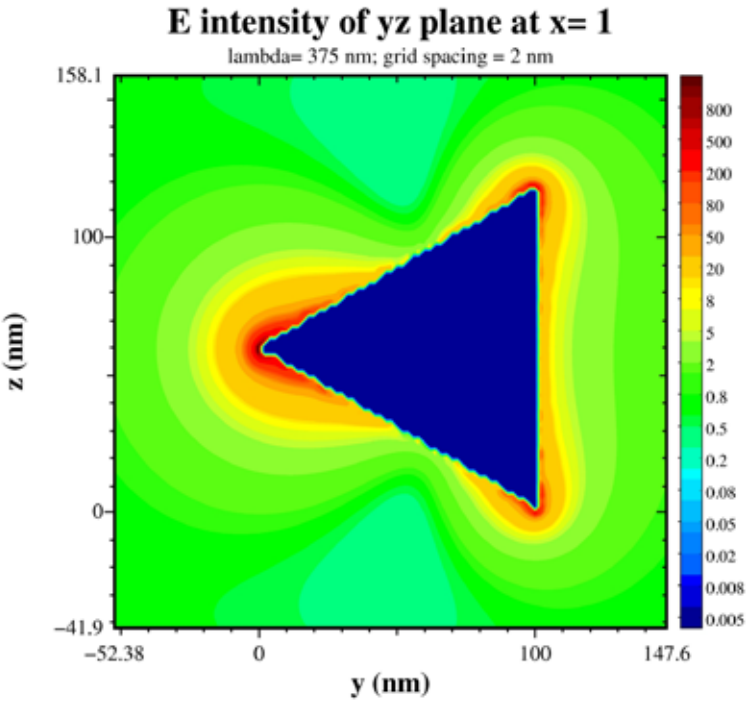

Figure 7. The electric field enhancement of the truncated tetrahedron in Figure 6(c). The calculation was made at the base of the tetrahedron. The maximum field enhancement is 3515.

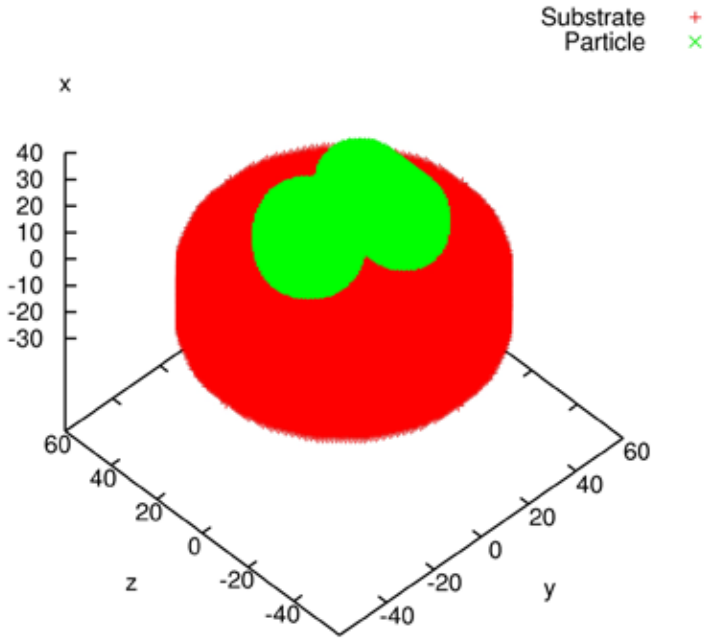

Figure 8. Dipole file for the substrate and particle configuration used in the SMSERS calculations. Two different polarizations were used. The light was polarized in the y-z plane with Polarization1 being at (*y,z*)=(1,1) and Polarization2 being (*y,z*)=(1,-1).

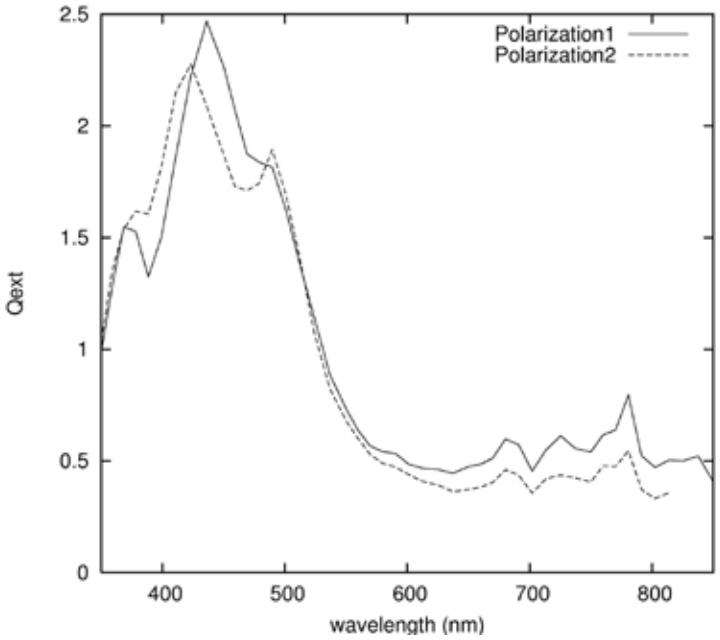

Figure 9. The extinction spectrum for the particle in Figure 8 for both polarizations.

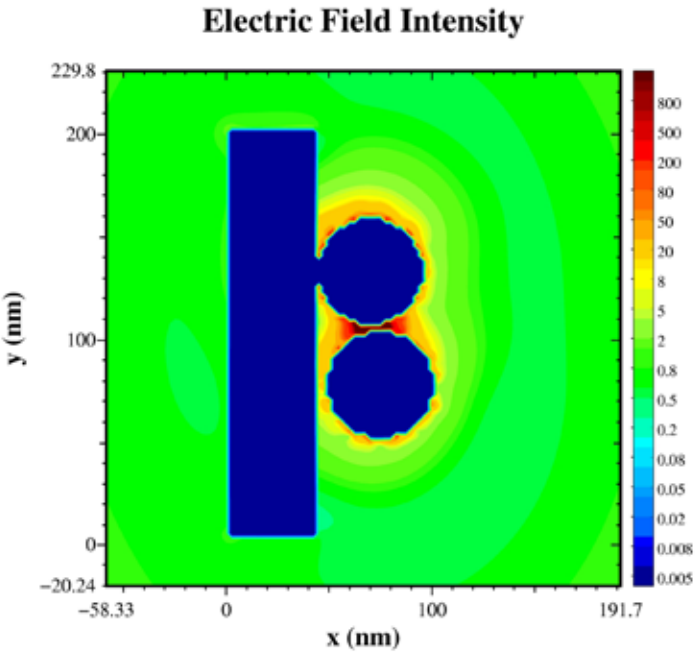

Figure 10. The electric field intensity of the particle described in Figure 8 at its plasmon wavelength. The plane is at *z*=85 nm. The maximum electric field enhancement is ~ 1.3 x 10^5.

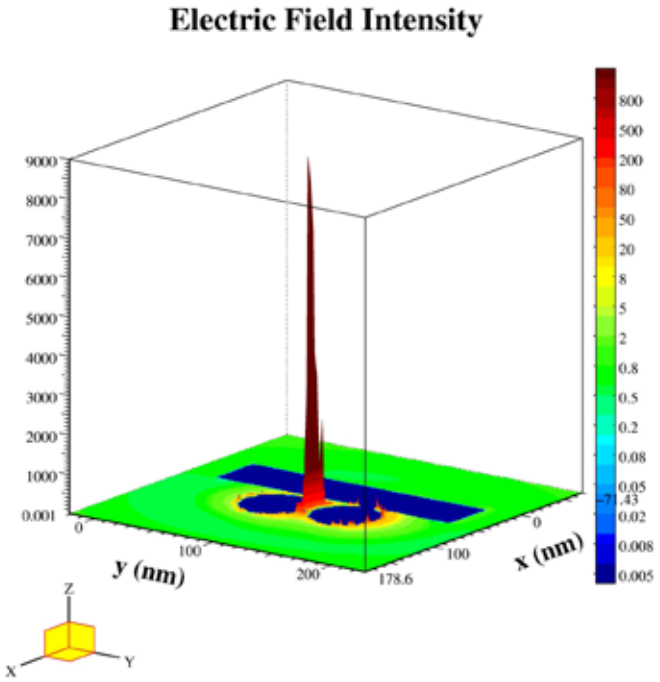

Figure 11. Electric field intensity for the same particle in Figure 8 at the plane *z*=85. The maximum intensity is E^2 ~ 1.3 x 10^5, but at a point which lies between two planes.

The extinction spectrum of the two polarizations in Figure 9 indicates that the particle is dependent on polarization for its effectiveness in SMSERS. Despite the seemingly small extinction value of the dimer configuration, the electric-field enhancement holds great promise for finding an active SMSERS particle. The localized electric-field enhancements of one polarization (Figures 10 and 11) were on the order of 10^5, which correlate with a SMSERS enhancement of 10^{10}. However, the other polarization experienced localized electric-field enhancements on the order of 10^4, so whether it would be useful in SMSERS is questionable. Also exciting is the position of the hot spot, which sits at the cusp — close to the junction but not exactly at it — for both polarizations.

Discussion

Analysis of the aluminum triangular prism and truncated tetrahedral results showed that the aluminum has a plasmon peak that lies in the ultraviolet part of the electromagnetic spectrum. The peak of the plasmon is tunable by changing the size parameters. With the triangular prisms, the larger the side length and thinner the prism, the more red-shifted the plasmon peak will be. Truncated tetrahedrons behaved similarly. The plasmon peak shifts more to the red the longer the sides and the larger the height. However, aspect ratio is crucial; the ratio must be large to obtain a good extinction factor. The aluminum particles are good field enhancers, sometimes reaching as high at ~10^4, which gives a SERS enhancement of 10^8. Implications of these results may be far reaching. This enhancement suggests that Al is a good potential SERS substrate and that SMSERS might be viable on an aluminum particle.

The ability to use more complex shapes is an exciting addition to the field of SMSERS. DDA analysis of experimental observation of the SMSERS-active junction in this study revealed large enhancement factors. Additionally, analysis of the accuracy of the SMSERS-active junction particles was not possible despite the agreement between the DDA shape file representation of simpler geometric shapes and their real-life counterparts. However, the preliminary results of the electric-field enhancement are promising. The localized electric-field enhancement was ~10^5, which corresponds to a SERS enhancement of 10^{10}. It has been theorized that electromagnetic enhancements of 10^9–10^{10} are needed before phenomena such as single-molecule SERS can be identified. The position of the field enhancement also provides information crucial to determine the possibility of SERS. The hot spot occurred where the two particles were extremely close but not touching. This is a more natural position for a single molecule to settle than the immediate junction of the two particles.

Conclusion

Three main topics were examined in this research: the creation of different methods to accurately model three-dimensional shapes; the possibility of using aluminum as an active SERS metal; and the examination of actual lab-fabricated particles for use in single-molecule SERS. Many successful routines were written to accurately model different particles and configurations. Single, free particles, configurations of particles, and particles resting on substrates were all effectively modeled.

The results show the promise of aluminum as an active SERS particle in the blue and ultraviolet regions of the electromagnetic spectrum. It provides the grounds for future work on aluminum to increase the electric-field enhancement and shift the plasmon peak farther into the visible light spectrum, which would make SERS much more viable.

The results of the SMSERS active junction experiments were very exciting. The electric-field enhancement at the plasmon peak was on the order of 10^5, the largest localized electric-field enhancement seen. An enhancement factor of this size correlates with a high probability of the particle being an active SERS particle. Future research will seek to emulate this result with great precision for applications in single-molecule SERS. Additional work will also look at how to incorporate different metals.

This research was supported primarily by the Nanoscale Science and Engineering Initiative of the National Science Foundation under NSF Award Number ***EEC-0647560.*** *Any opinions, findings and conclusions or recommendations expressed in this material are those of the author(s) and do not necessarily reflect those of the National Science Foundation.*

References

(1) Nie, S.; *Emory S. R. Science*. **1997,** *275,* 110–1106.

(2) Malinsky, M. D.; Kelly, K. L.; Schatz, G. C. Van Duyne,, R. P., *J. Phys. Chem. B* **2001,** *105,* 2243–2350.

(3) Hao, E; Schatz, G. C. *J. Chem. Phys.* **2004,** *120,* 357–366.

(4) Borhen, C. F.; Huffman, D. R. *Absorption and Scattering of Light by Small Particles.* Wiley-VCH: Mörlenbach, **2004.**

(5) Mie, G. *Ann. Phys.* **1908,** *25,* 377–445.

(6) Purcell, E. M.; Pennypacker, C. R. *Astrophys. J.* **1973,** *186,* 705.

(7) Draine, B. T.; Flatau, P. J. J. *Opt. Soc. Am. A* **1994,** *11,* 1491–1499.

(8) Raman, C. V.; Krishnan, K. S. *Nature*. **1928,** *121,* 501–502.

(9) Micic, M.; Klymyshyn, N.; Suh, Y. D.; Lu, H. P. *J. Phys. Chem. B* **2003,** *107,* 1574–1584.

(10) Xu, H.; Aizpurua, J.; Käll, M.; Apell, P. *Phys. Rev. E* **2000,** *62,* 4318–4324.

(11) Yang, W.; Schatz, G. C.; Van Duyne, R. P. J. *Chem. Phys.* **1995,** *103,* 869–875.

(12) Jensen, T. R.; Schatz, G. C.; Van Duyne, R. P. *J. Phys. Chem. B* **1999,** *203,* 2394–2401.

(13) Draine, B. T. *Astrophys. J.* **1988,** *333,* 848–872.

(14) Program DDSCAT by B. T. Draine and P. J. Flatau, University of California, San Diego, Scripps Institute of Oceanography.

(15) Jin, R.; Cao, W.; Mirkin, C. A.; Kelly, K. L.; Schatz, G. C.; Zheng, J. G. *Science.* **2001,** *294,* 1901–1903.

(16) Johnson, P. B.; Christy, R. W.; *Phys. Rev. B* **1972,** *6,* 4370–4379.

(17) Lide, D. R. *CRC Handbook of Chemistry and Physics;* CRC Press: New York, **2000:** 12.133–12.156